Original Research Article

Power Law Fluid Model for Thermal Elastohydrodynamic Lubrication

Abstract

The aim of this paper is to analyse thermal elastohydrodynamic lubrication (TEHL) of rolling a bearing using a non-Newtonian fluid that is described by the power law model. The performance characteristics of the rolling bearing are determined for various flow non-Newtonian flow index for dilatant, Newtonian and pseudo plastic fluids. The one-dimensional Reynolds and energy equations are both modified to incorporate the non-Newtonian nature of the lubricant. The coupled system of governing equations are discretized using the finite difference method and solved simultaneously. The results show that the pressure, film thickness and temperature for dilatant fluids increased with increase in the flow index as compared to pseudo plastic fluids. The influence of thermal effects on pressure and film thickness is more significant compared with that under isothermal elastohydrodynamic lubrication (EHL) especially on the case of dilatant fluids. The viscosity of the lubricant increases with increase in pressure and reduces with increment in temperature. The surface roughness increases the film thickness of the lubricant. The fluid pressure, film thickness and temperature increases with increase in the bearing speed. To truly reflect the characteristics of EHL models, thermal effects should be considered.

Keywords: Elastohydrodynamic, Power Law, Film Thickness, Thermal.

1 Introduction

Modern machine elements need to be efficient in order to meet the demands in the manufacturing process. Most of these machines use rolling bearings which have lubricants separating the surfaces in motion. These machines depend on lubrication to keep the bearings turning. The high speeds in rolling bearings cause energy dissipation due to shearing which causes increase in the temperature of the fluid. This reduces the viscosity and pressure of the lubricant leading to wear and tear. The isothermal theory is popularly used in EHL modelling. However, the industrial requirements such as increase in speed and load generate thermal effects which can no longer be neglected. Elastohydrodynamic lubrication (EHL) is a type of lubrication that occurs in thin films and high pressure in many mechanical components such as cams, gears, rolling bearings, and many more. This type of lubrication results to deformation of the surfaces in contact. It normally occurs when non-conforming contacts suffer from elastic strains.
Additives are mainly chemical compounds that improve the lubrication properties. The introduction of additives to improve the viscosity of lubricants is vital [1]. This changes the

linear relationship between the shear rate and shear stress making the lubricant to become non-Newtonian. The use of lubricants which are non-Newtonian has become a global phenomenon in modern industrial operations. The research study [2] noted that the non-Newtonian model for sliding conditions yielded better results when compared to experimental works in EHL.
The study [3], noted that under elastohydrodynamic lubrication most lubricants exhibit the non-Newtonian nature. The non-Newtonian nature of lubricants behaviour has been developed using various rheological models. The models that have been analysed and developed include the Eyring model, power law model, Maxwell model, Johnson-Tevaarwerk model among others [4,5]. Most researchers have recommended the power law model for traction studies and lubrication. And it has been consistently been used in most elastohydrodynamic research [6]. This is because the power law model accurately characterizes the dilatant and pseudo plastic fluids which characterizes the shear thickening and shear thinning of lubricants respectively which are both non-Newtonian, [7,8]. The power law model is mostly preferred in because of its mathematical simplicity and its wide coverage when it comes to the analysis of lubricants.
The surface of the bearing during the manufacturing phase is not perfectly smooth. Under strong magnification, ridges are observed which bring the aspect of surface roughness in the bearing. Under high pressure and load, the film may thin and be compared to the surface roughness which may result to friction. Therefore, understanding how the surface roughness affects the pressure and temperature distribution which in turn affects the film thickness is important in EHL studies [9]. The study noted that the surface roughness increase resulted to increase in both the pressure, temperature and the film thickness of the lubricant.
Elastohydrodynamic lubrication experiments still remain expensive and time consuming to conduct. Thus, mathematical numerical simulations come in handy. The finite difference method is preferred as a numerical tool because of its simple approximation of the derivatives as demonstrate in the research [10]. The study [11] also used the finite difference method to solve the two-dimensional Reynolds-Eyring and obtained excellent results. The surface roughness, high speeds and high temperature influences the rheology of the lubricant [12]. Thus, thermal effects which affect the viscosity of the lubricant and the performance of the bearing can no longer be neglected. The research [13] solved both the Reynolds and energy equation and demonstrated that thermal effects, affect the viscosity and density of the lubricant.
This study aims to better predict the non-Newtonian behaviour of the film in bearings operating under more thermal conditions.In this paper, a one-dimensional modified Reynolds equation that incorporates the non-Newtonian nature of the lubricant using the power law model is derived. This helped in simplification of the computational complexity and improvement of the solution efficiency. The thermodynamic aspect of the problem is considered by incorporating the energy equation and the viscosity and density dependence on both the pressure and temperature. The influence of power index values on pressure, film thickness and temperature of the fluid are analysed for isothermal and thermal cases. The viscosity of lubricant, speed and surface roughness properties of the rolling bearing are also analysed.

2 Geometry of the Model

The elastohydrodynamic problem can be reduced to a contact of a roller and a flat surface. Figure 1, shows the contact geometry where the lubricant is taken to obey the power law.

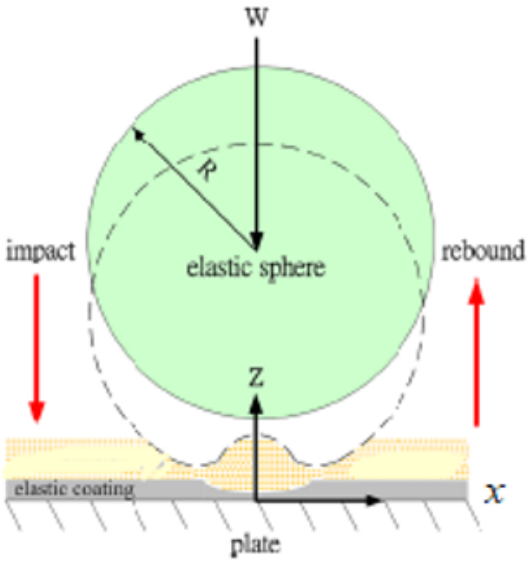

Figure 1: Geometry of the model.

3 Governing Equations

3.1 Power Law Model

The non-Newtonian nature of the lubricant is modelled using the power law for the thermal elastohydrodynamic lubrication. The tensors for stress and strain for the power law model are related according [14]

$$\tau = \eta \left| \frac{\partial u}{\partial z} \right|^{n-1} \frac{\partial u}{\partial z}. \tag{1}$$

The conditions for $n < 1$, correspond to pseudo plastic fluid, $n = 1$ correspond to Newtonian fluid and $n > 1$ correspond to dilatant fluid [15].

3.2 Modified Reynolds Equation

The film thickness in the model is thin hence the body forces and inertia forces can be neglected. The momentum equation in the x-direction reduces to,

$$\frac{\partial p}{\partial x} = \frac{\partial \tau}{\partial z}. \tag{2}$$

Substituting Equation 1 into Equation 2 we obtain,

$$\frac{\partial p}{\partial x} = \frac{\partial}{\partial z} \left(\eta \left| \frac{\partial u}{\partial z} \right|^{n-1} \frac{\partial u}{\partial z} \right). \tag{3}$$

Assuming that the pressure distribution is only along the x-direction, Equation 3 can be partially integrated with respect to z alone with C_1 a constant of integration to obtain the following result,

$$\eta \mid \frac{\partial u}{\partial z} \mid^{n-1} \frac{\partial u}{\partial z} = \frac{\partial p}{\partial x} z + C_1. \tag{4}$$

Assuming that $\left|\ \frac{\partial u}{\partial z}\ \right|$ is positive and making $\frac{\partial u}{\partial z}$ the subject of the formula from Equation 4. Now partially integrating u with respect to z with C_2 as a constant of integration to obtain,

$$u = \eta^{-\frac{1}{n}} \left(\frac{n}{n+1}\right) \frac{1}{\frac{\partial p}{\partial x}} \left(\frac{\partial p}{\partial x} z + C_1\right)^{\frac{n+1}{n}} + C_2. \tag{5}$$

Applying the boundary condition at $z = 0$; $u = U_1$ on the lower plate, Equation 5 becomes,

$$U_1 = \eta^{-\frac{1}{n}} \left(\frac{n}{n+1}\right) \frac{1}{\frac{\partial p}{\partial x}} (C_1)^{\frac{n+1}{n}} + C_2. \tag{6}$$

Now, making the value of C_2 the subject of the formulae from Equation 6 and substituting it in Equation 5, we obtain,

$$u = U_1 + \eta^{-\frac{1}{n}} \left(\frac{n}{n+1}\right) \frac{1}{\frac{\partial p}{\partial x}} \left[\left(\frac{\partial p}{\partial x} z + C_1\right)^{\frac{n+1}{n}} - (C_1)^{\frac{n+1}{n}}\right]. \tag{7}$$

Now, partially integrating Equation 7 with respect to u yields

$$\frac{\partial u}{\partial z} = \eta^{-\frac{1}{n}} [\left(\frac{\partial p}{\partial x} z + C_1\right)^{\frac{n+1}{n}}. \tag{8}$$

Applying the boundary condition at

$$z = \frac{h}{2}, \qquad \frac{\partial u}{\partial z} = 0,$$

We obtain

$$C_1 = -\frac{\partial p}{\partial x} \frac{h}{2}. \tag{9}$$

Substituting Equation 9 into Equation 7, we obtain,

$$u = U_1 + \eta^{-\frac{1}{n}} \left(\frac{n}{n+1}\right) \frac{1}{\frac{\partial p}{\partial x}} \left[\left(\frac{\partial p}{\partial x} z - \frac{\partial p}{\partial x} \frac{h}{2}\right)^{\frac{n+1}{n}} - \left(-\frac{\partial p}{\partial x} \frac{h}{2}\right)^{\frac{n+1}{n}}\right]. \tag{10}$$

Rearrangement

$$u = U_1 + \eta^{-\frac{1}{n}} \left(\frac{n}{n+1}\right) \left(\frac{\partial p}{\partial x}\right) \left|\frac{\partial p}{\partial x}\right|^{\frac{1-n}{n}} \left[\left(\frac{h}{2}\right)^{\frac{n+1}{n}} - \left(\frac{h}{2} - z\right)^{\frac{n+1}{n}}\right]. \tag{11}$$

Applying the boundary condition at $z = h$, $u = U_2$ on upper plate on Equation 11 to obtain,

$$U_2 = U_1 + \eta^{-\frac{1}{n}} \left(\frac{n}{n+1}\right) \left(\frac{\partial p}{\partial x}\right) \left|\frac{\partial p}{\partial x}\right|^{\frac{1-n}{n}}. \tag{12}$$

Rearranging Equation 12, to obtain

$$U_2 - U_1 = \eta^{-\frac{1}{n}} \left(\frac{n}{n+1}\right) \left(\frac{\partial p}{\partial x}\right) \left|\frac{\partial p}{\partial x}\right|^{\frac{1-n}{n}}. \tag{13}$$

The one-dimensional continuity is given by,

$$\frac{\partial \rho}{\partial t} + \frac{\partial (\rho u)}{\partial x} = 0. \tag{14}$$

Now, substituting the value of u from Equation 11 into Equation 14, yields

$$\frac{\partial \rho}{\partial t} + \frac{\partial}{\partial x}\left[U_1 + \eta^{-\frac{1}{n}}\left(\frac{n}{n+1}\right)\left(\frac{\partial p}{\partial x}\right)\left|\frac{\partial p}{\partial x}\right|^{\frac{1-n}{n}}\left[\left(\frac{h}{2}\right)^{\frac{n+1}{n}} - \left(\frac{h}{2}-z\right)^{\frac{n+1}{n}}\right]\right] = 0. \tag{15}$$

Integrating partially with respect to z from $z = 0$ to $z = h$ and using Equation 13, Equation 15 becomes,

$$\frac{\partial \rho h}{\partial t} - \frac{\partial}{\partial x}\left[\rho\eta^{-\frac{1}{n}}\left(\frac{2n}{2n+1}\right)\left(-\frac{\partial p}{\partial x}\right)\left|\frac{\partial p}{\partial x}\right|^{\frac{1-n}{n}}\left[\left(\frac{h}{2}-z\right)^{\frac{2n+1}{n}} - \left(\frac{h}{2}\right)^{\frac{2n+1}{n}}\right]\right] + \frac{\partial}{\partial x}\left[\frac{u_1+U_2}{2}\rho h\right] = 0. \tag{16}$$

Taking the average velocity $U_m = U_1 + U_2$ and considering unsteady flow of lubricant Equation 16 becomes,

$$\frac{\partial}{\partial x}\left[\rho\eta^{-\frac{1}{n}}\left(\frac{2n}{2n+1}\right)\left(-\frac{\partial p}{\partial x}\right)\left|\frac{\partial p}{\partial x}\right|^{\frac{1-n}{n}}\left[\left(\frac{h}{2}-z\right)^{\frac{2n+1}{n}} - \left(\frac{h}{2}\right)^{\frac{2n+1}{n}}\right]\right] = \frac{u_m}{2}\frac{\partial(\rho h)}{\partial x} + \frac{\partial \rho h}{\partial t}. \tag{17}$$

3.3 Energy equation

Due to friction of the rolling bearing, thermal effects are considered. The energy equation in one dimensional is given by [16],

$$\rho C_p\left(u\frac{\partial \theta}{\partial x}\right) = k\left(\frac{\partial^2 \theta}{\partial x^2}\right) + \eta\left|\frac{\partial u}{\partial z}\right|^{n-1}\left(\frac{\partial u}{\partial z}\right)^2. \tag{18}$$

3.4 Film Thickness Equation

The film thickness equation considers both the surface roughness and deformations of the bodies in contact. Thus, the film thickness according to [17] is given by,

$$h(x) = h_{00} + \frac{x^2}{2R} + s_r(x) - \frac{2}{\pi E'}\int_{in}^{out} ln\left|x - x'\right| p(x')dx'. \tag{19}$$

3.5 The Load Equation

The sum of pressures in the lubricant in the flow field are balanced by the external force. Thus, the load balance equation according to the study [18] is given by,

$$\int_{in}^{out} p(x)\, dx = W. \tag{20}$$

3.6 Viscosity dependence pressure and temperature

The lubricant's viscosity is affected by both pressure and temperature. This relationship according to the research [19] is given by,

$$\eta = \eta_0 \exp\left[[ln(\eta_0) + 9.67]\left(-1 + (1 + 5.1 * 10^{-}9p)^Z\right)\left(\frac{\theta - 138}{\theta_0 - 138}\right)^{-S}\right]. \tag{21}$$

3.7 Density dependence pressure and temperature

The compressibility of the lubricant is affected by both pressure and temperature. This relation described by the research [19] is given by,

$$\rho = \rho_0 \left[1 + \frac{0.6 * 10^{-}9p}{1 + 1.7 * 10^{-}9p} - 0.00065\,(\theta - \theta_0)\right]. \tag{22}$$

3.8 Non Dimensionalization

The equations are non-dimensionalized using the Hertzian dry contact variables below [20] .

$$\bar{\rho} = \frac{\rho}{\rho_0}, \bar{\eta} = \frac{\eta}{\eta_0}, X = \frac{x}{a}, Y = \frac{y}{a}, P = \frac{p}{p_h}, H = \frac{hR}{a^2}, T = \frac{tU_m}{2a},$$
$$H_{00} = \frac{h_{00}R}{a^2}, \bar{\theta} = \frac{\theta}{\theta_0}, U = \frac{u\eta_0}{RE'}, V = \frac{v\eta_0}{RE'}.$$

The modified Reynolds Equation 17 in dimensionless form is given by

$$\frac{\partial}{\partial X}\left[\beta\left(\frac{\partial P}{\partial X}\right)\left|\frac{\partial P}{\partial X}\right|^{\frac{1-n}{n}}\right] = \lambda\left[\frac{\partial \overline{\rho} H}{\partial X} + \frac{\partial \overline{\rho} H}{\partial T}\right], \tag{23}$$

with

$$\beta = \frac{\overline{\rho} H^{\frac{2n+1}{n}}}{\overline{\eta}^{\frac{1}{n}}} \quad \lambda = 2^{\frac{2n+1}{n}}\left(\frac{2n+1}{2n}\right)\left(\frac{UR}{a^2}\right)\left(\frac{\eta_0 R}{a p_h}\right)^{\frac{1}{n}}.$$

Assuming the change of pressure is always positive Equation 23 becomes

$$\frac{\partial}{\partial X}\left[\beta\left(\frac{\partial P}{\partial X}\right)^{\frac{1}{n}}\right] = \lambda\left[\frac{\partial \overline{\rho} H}{\partial X} + \frac{\partial \overline{\rho} H}{\partial T}\right]. \tag{24}$$

The energy Equation 18 in dimensionless form is given by

$$\overline{\rho}\rho_0\left[\frac{\theta_0 E' R}{a\eta_0}\left(U\frac{\partial \overline{\theta}}{\partial X}\right)\right] = k\frac{\theta_0}{a^2}\frac{\partial^2 \overline{\theta}_0}{\partial X^2} + \overline{\eta}\eta_0\left|\frac{\partial U}{\partial Z}\right|^{n-1}\left(\frac{\partial U}{\partial Z}\right)^2. \tag{25}$$

The film thickness Equation 19 after non-dimensionalization becomes

$$H(X) = H_{00} + \frac{X^2}{2} + S_R(X) - \frac{1}{\pi}\int_{in}^{out} ln\left|X - X'\right| P(X')dX'. \tag{26}$$

The load Equation 20 after non-dimensionalization becomes

$$\int_{in}^{out} P(X)\,dX = \frac{\pi}{2}. \tag{27}$$

Equation 21 after non-dimensionalization becomes,

$$\overline{\eta} = \exp\left[[ln(\eta_0) + 9.67]\left(-1 + (1 + 5.1 * 10^{-}9Pp_h)^Z\right)\left(\frac{\overline{\theta}\theta_0 - 138}{\theta_0 - 138}\right)^{-S}\right]. \tag{28}$$

Equation 22 in dimensionless form is given by

$$\overline{\rho} = \left[1 + \frac{0.6 * 10^{-}9Pp_h}{1 + 1.7 * 10^{-}9Pp_h} - 0.00065\,\theta_0(\overline{\theta} - 1)\right]. \tag{29}$$

3.9 Boundary Conditions

The TEHL equations are discretised on a rectangular domain $X_{in} \leq X \leq X_{out}$. Thus, the boundary conditions are,

$$P(X_{in}) = 0 \quad P(X_{end}) = 0 \quad \frac{\partial P}{\partial X_{end}} = 0,$$
$$\theta(X_{in}) = \theta(X_{out}) = \theta_0.$$

3.10 Numerical Solution

The Modified Reynolds and energy equations are non-linear partial differential equations. These equations are discretised using the explicit finite difference scheme at finite sized nodes. The domain of the problem is divided into 51 nodes along the rolling bearing direction X. Equation 24 in discrete form is given by

$$\frac{\beta_{i+\frac{1}{2}} \left(P_{i+1} - P_i\right)^{\frac{1}{n}} - \beta_{i-\frac{1}{2}} \left(P_i - P_{i-1}\right)^{\frac{1}{n}}}{(dx)^{\frac{n+1}{n}}},$$

with

$$\beta_{i+\frac{1}{2}} = \frac{2}{\frac{1}{\beta_{i+1}} + \frac{1}{\beta_i}} \quad \beta_{i-\frac{1}{2}} = \frac{2}{\frac{1}{\beta_i} + \frac{1}{\beta_{i-1}}}.$$

In solving Equation 24 numerically assuming a steady flow, an equation system is formed in form of matrix for $i = 1, 2, 3, ..., N+1$, given by

$$\begin{bmatrix} 1 & & & & & & & & \\ -\beta_{i-\frac{1}{2}} & \beta_{i+\frac{1}{2}} & & & & & & & \\ & -\beta_{i-\frac{1}{2}} & \beta_{i+\frac{1}{2}} & & & & & & \\ & & -\beta_{i-\frac{1}{2}} & \beta_{i+\frac{1}{2}} & & & & & \\ & & \ddots & \ddots & \ddots & \ddots & & & \\ & & & & & -\beta_{i-\frac{1}{2}} & \beta_{i+\frac{1}{2}} & & \\ & & & & & & -\beta_{i-\frac{1}{2}} & \beta_{i+\frac{1}{2}} & \\ & & & & & & & & 1 \end{bmatrix} \begin{bmatrix} P_0 \\ (P_1 - P_0)^{\frac{1}{n}} \\ (P_2 - P_1)^{\frac{1}{n}} \\ (P_3 - P_2)^{\frac{1}{n}} \\ (P_4 - P_3)^{\frac{1}{n}} \\ \vdots \\ (P_{N-1} - P_{N-2})^{\frac{1}{n}} \\ (P_N - P_{N-1})^{\frac{1}{n}} \\ P_N \end{bmatrix} =$$
$$\frac{\lambda}{dx} \begin{bmatrix} 0 \\ H_1\overline{\rho}_1 - H_0\overline{\rho}_0 \\ H_2\overline{\rho}_2 - H_1\overline{\rho}_1 \\ H_3\overline{\rho}_3 - H_2\overline{\rho}_2 \\ H_4\overline{\rho}_4 - H_3\overline{\rho}_3 \\ \vdots \\ H_{N-1}\overline{\rho}_{N-1} - H_{N-2}\overline{\rho}_{N-2} \\ H_N\overline{\rho}_N - H_{N-1}\overline{\rho}_{N-1} \\ 0 \end{bmatrix}. \tag{30}$$

The energy equation in discrete form is given by

$$\overline{\theta}_i = \left[\overline{\rho}\rho_0 C_p \left(\frac{\theta_0 E' R}{a\eta_0} \left(U_i \frac{\overline{\theta}_{i+1}}{dX}\right)\right) - \frac{k\theta_0}{a^2} \left(\frac{\overline{\theta}_{i+1} + \overline{\theta}_{i-1}}{(dX)^2}\right) - \overline{\eta}_i \eta_0 \left|\frac{\partial U}{\partial Z}\right|^{n-1} \left(\frac{\partial U}{\partial Z}\right)^n\right] \div \left[\overline{\rho}_i \rho_0 \left(\frac{\theta_0 E' R}{a\eta_0} \left(\frac{U_i}{dX}\right)\right) - \frac{2k\theta_0}{a^2 (dX)^2}\right], \tag{31}$$

with

$$\frac{\partial U}{\partial Z} = (\overline{\eta}_i \eta_0)^{-\frac{1}{n}} \left(\frac{aH^2 p_h}{2R}\right)^{\frac{1}{n}} \left(\frac{\partial P}{\partial Z}\right) \left|\frac{\partial P}{\partial Z}\right|^{\frac{1-n}{n}}.$$

Film thickness equation in discrete form

$$H(X) = H_{00} + \frac{{X_i}^2}{2} + S_{Ri} - \frac{1}{\pi}\sum_{j=1}^{N} K_{i,j} P(X_j), \tag{32}$$

where

$$K_{i,j} = \left(X_i - X_j + \frac{dx}{2}\right)\left(ln\left|X_i - X_j + \frac{dx}{2}\right| - 1\right) - \left(X_i - X_j - \frac{dx}{2}\right)\left(ln\left|X_i - X_j - \frac{dx}{2}\right| - 1\right).$$

The load equation in discrete form

$$dX \sum_{i=1}^{N} \left(\frac{P_{i+1} - P_i}{2}\right) - \frac{\pi}{2} = 0. \tag{33}$$

Lubricant viscosity equation in discrete form

$$\overline{\eta}_i = \exp\left[[ln(\eta_0) + 9.67]\left(-1 + (1 + 5.1 * 10^{-}9 P_i p_h)^Z\right)\left(\frac{\overline{\theta}_i \theta_0 - 138}{\theta_0 - 138}\right)^{-S}\right]. \tag{34}$$

Lubricant density equation in discrete form

$$\overline{\rho}_i = \left[1 + \frac{0.6 * 10^{-}9 P_i p_h}{1 + 1.7 * 10^{-}9 P_i p_h} - 0.00065\,\theta_0(\overline{\theta}_i - 1)\right]. \tag{35}$$

Table 1: Computational data

Radius of rolling element(m)	0.014
Load(N)	2.8×10^{-8}
Hertzian radius (m)	0.012
Hertzian pressure(Pa)	6.8×10^{-3}
Average speed(m/s)	1.8
Density at reference pressure (kg/m^3)	846
Reference temperature (K)	300
Viscosity at ambient pressure($Pa.s$)	0.14
Elastic modulus(Pas)	0.02
Specific heat capacity (J/Kg K)	460
Thermal conductivity(W/m K)	0.9
Central film thickness (m)	1×10^{-4}
Surface roughness (m)	0.002
Temperature viscosity constant	0.2

4 Results and Discussion

In Table 1, the bearing and lubricant properties for the present study are listed. The discretised equations together with the boundary conditions are coupled together and solved numerically using the Gauss-Seidel iteration method with the help of MATLAB. Various pressure, film thickness and temperature profiles for various flow parameters were obtained as follows;

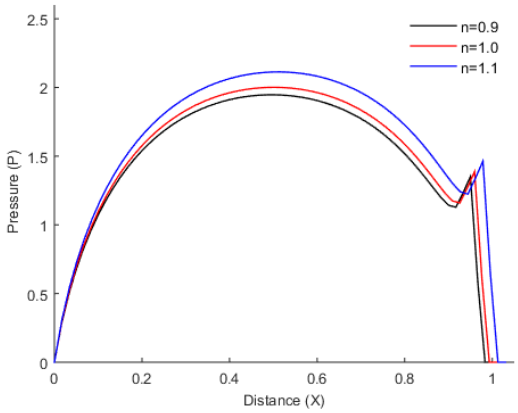

Figure 2: Effects of flow index on fluid pressure.

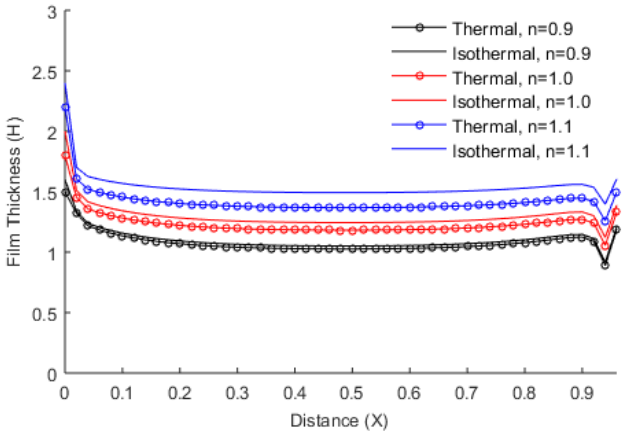

Figure 5: Effects of flow index on film thickness for isothermal and thermal cases.

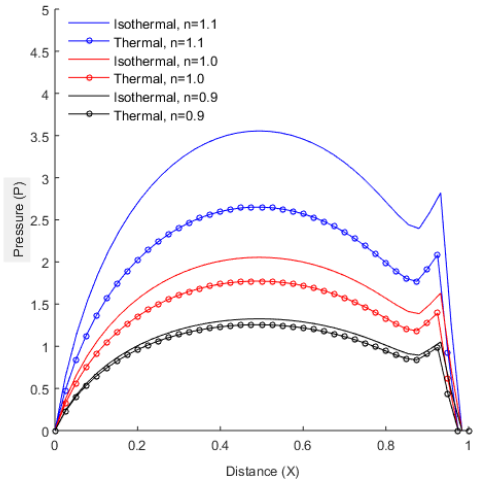

Figure 3: Effects of flow index on fluid pressure for isothermal and thermal cases.

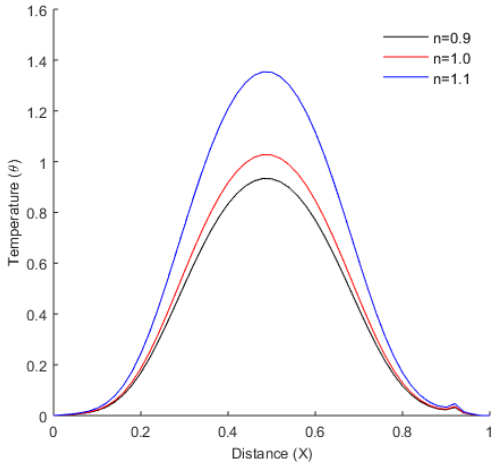

Figure 6: Effects of flow index on fluid temperature.

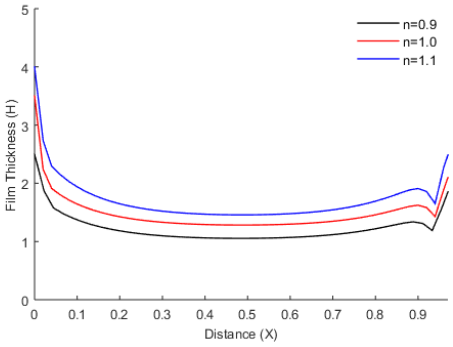

Figure 4: Effects of flow index on film thickness.

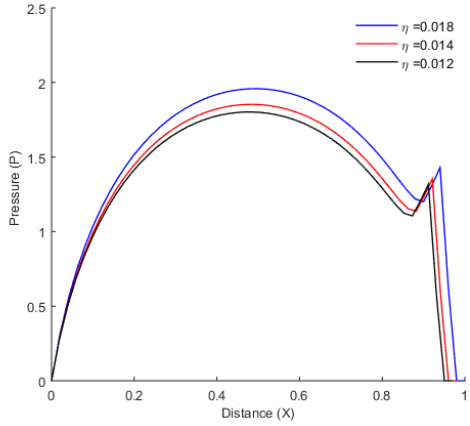

Figure 7: Effects fluid pressure on viscosity.

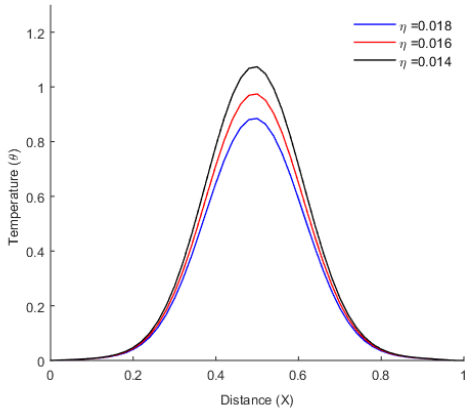

Figure 8: Effects of fluid temperature on viscosity.

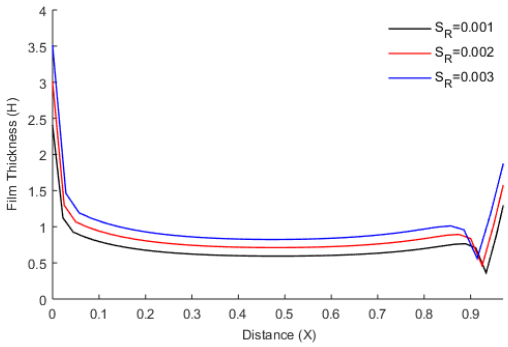

Figure 9: Effects of surface roughness film thickness.

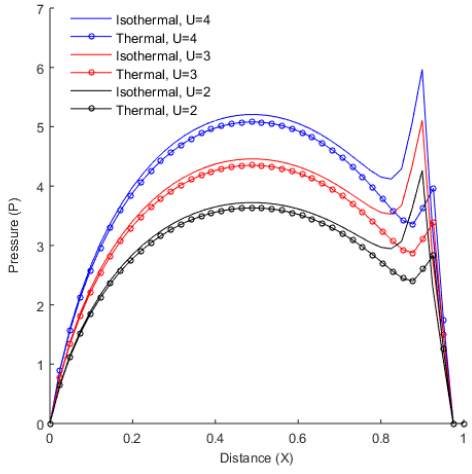

Figure 10: Effects of bearing speed on fluid pressure for isothermal and thermal cases.

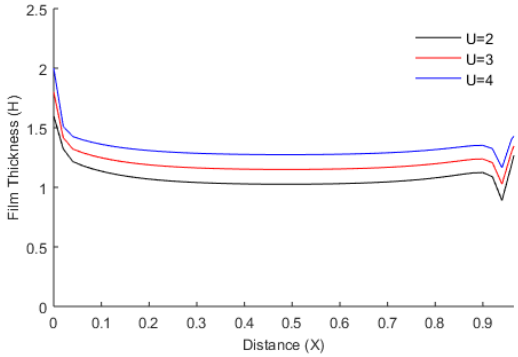

Figure 11: Effects of bearing speed on film thickness.

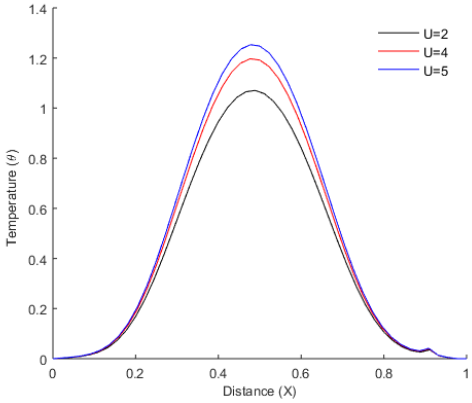

Figure 12: Effects of bearing speed on fluid temperature.

The lubrication behaviour of the bearing characteristics depends on the flow index. The values of n are assumed to take the values of 1.1 for dilatant, 1.0 for Newtonian and 0.9 for pseudo plastic lubricants. The film pressure increases with increase in the flow index n as illustrated by Figure 2. The fluid pressure is higher for dilatant fluids than that of Newtonian and pseudo plastic fluids. The pressure is also noted to increase gradually to maximum at the contact and then decreases gradually. The pressure peak at the exit of the bearing is due to cavitation property of the lubricant.

Figure 3 illustrates the film pressure profiles for different values of flow index and for different cases of isothermal and thermal EHL. The pressure variations between isothermal and thermal cases also increase with increase in the flow index. It is also noted that thermal effects are more important in dilatant fluids where the variations of the pressure profiles between the isothermal and thermal cases are higher than the other two cases. The variation of differences in isothermal and thermal cases in pseudo plastic fluids is very small.

Figure 4 illustrates the film thickness profiles for different values of the flow index. The film thickness forms a U-shaped region due the pressure gradient. The film thickness increases with increase in the flow index. This is because a larger flow index means a larger effective viscosity and stronger shear thickening ability of the fluid hence a stronger oil film carrying capacity. The variation of the film thickness between isothermal and thermal cases also increase with increase in the flow index. As earlier seen in pressure cases, thermal effects are more predominant in dilatant fluids as compared to Newtonian and pseudo plastic fluids.

Figure 5 illustrates the film film thickness profiles for different values of flow index and for different cases of isothermal and thermal EHL. The film thickness variations between isothermal and thermal cases also increase with increase in the flow index. It is also noted that thermal effects are more important in dilatant fluids where the variations of the film thickness profiles between the isothermal and thermal cases are higher than Newtonian and pseudoplastic fluids. The variation of differences in isothermal and thermal cases in pseudo plastic fluids is very small since they are not greatly affected by changes in temperature because of their shear thinning nature.

Figure 6 illustrate the temperature profiles for different flow index. The temperature increases steadily and reaches maximum at the contact centre, then decreases gradually. It is observed that the temperature profiles increase with increase in the flow index. However, the temperature profile for dilatant fluid is higher than that of Newtonian and pseudo plastic fluids. The shear thinning property of pseudo plastic fluids helps in heat transfer efficiency which results to minimal temperature changes as compared to dilatant fluids. That bearings that work under high temperatures a pseudo plastic lubricant should be considered since it has minimum effects on thermal effects changes.

The viscosity of the lubricant increases with pressure but reduces with increase in temperature as illustrated by Figures 7 and 8. The viscosity increases with increase in pressure due to compression of the lubricant which reduces its volume. Thus, the molecules of the lubricant move less freely hence the frictional forces increases which increase its viscosity. Increasing the temperature increases the kinetic energy of the lubricant molecules which make them move freely. The attractive binding cohesive forces of the molecules are therefore reduced which results to a reduction in the viscosity.

The surface roughness enhances the film thickness as demonstrated in Figure 9. This is due to the surface roughness affecting the viscosity of the lubricant. The viscosity of the lubricant is much higher in rough surfaces due to the pressure increase.

Figure 10 illustrate the effects of bearing speed on pressure for both isothermal and thermal cases. The pressure spike aptitude under isothermal EHL is higher than that of thermal EHL. The pressure spike amplitude of the thermal EHL are sensitive to the contact speed. This is s a result of reduction in the film thickness in thermal EHL as compared to isothermal EHL.

Figures 11 and 12 illustrate the effects of bearing speed on film thickness and fluid temperature. The film thickness and temperature of the lubricant increases with increase in speed. The film thickness increases due to increase in fluid pressure under high speeds. The temperature of the fluid increases with increase in speed because of viscous shearing due to frictional force. Thus, it is important to consider the influence of drop on contact speed on the film thickness when it comes to sudden breaking conditions in order to avoid dry contact of the bearing surfaces due too thinning of the lubricant.
The numerical findings on TEHL were compared with others that were modelled using the power law non-Newtonian model. The results are with reasonable agreement with research done by Prasad [21], Huo et. al [22] and Nessil et. al [23]

5 Conclusion

The research studied thermal elastohydrodynamic lubrication using the power law fluid model with surface roughness. The pressure, film thickness and temperature of the fluid all increases with increase in the flow index. Dilatent fluids are greatly affected by temperature changes as compared to Newtonian and pseudo plastic fluids. The pressure distribution for both pressure and film thickness are higher for isothermal than thermal case. The viscosity of the lubricant increases with pressure but reduces with increase in temperature. This is because the viscosity of the lubricant is smaller for thermal case than for the isothermal case. The film thickness increases with increase in surface roughness. The fluid pressure, film thickness and temperature increases with increase in bearing speed. The research has demonstrated the importance of thermal effects on EHL. Thus, thermal effects should be considered to truly reflect the behaviour and characteristics of EHL models.

Nomenclature

ρ	Density(kg/m^3)
ρ_0	Density at reference pressure(kg/m^3)
n	Flow index
θ	Temperature(K)
θ_0	Reference temperature(K)
p	Pressure(Pas)
p_h	Hertzian Pressure(Pa)
h	Film thickness(m)
h_{00}	central film thickness
$E^{'}$	Elastic modulus(Pa)
a	Hertzian contact radius(m)
u_m	average speed(m/s)
R	Radius of rolling element(m)
t	Time(s)
s_r	Surface roughness(m)
x	Distance along rolling direction(m)
dx	Space step in x axis(m)
dt	Time step(s)
X	Dimensionless distance
w	Load(N)
C_p	Specific heat capacity(J/kg K)

k	Thermal conductivity(W/m K)
η	Viscosity of lubricant($Pa.s$)
η_0	Viscosity at ambient pressure($Pa.s$)
$\overline{\eta}$	Dimensionless viscosity
i	Grid nodes in x direction
Z	Pressure-viscosity constant
S	Temperature viscosity constant

Data Availability

The data used to support the findings of this study are available from the corresponding author upon request.

References

[1] S.I. Shara, E.A. Eissa and J.S. Basta, " Polymers additive for improving the flow properties of lubricating oil," *Egyptian journal of petroleum*, volume 27, issue 4, pp. 795-799, 2018.

[2] J. Xie and Y.C. Jin, " Parameter determination for the Cross-rheology equation and its application to modeling non-Newtonian flows using the WC-MPS method," *Engineering Applications of Computational Fluid Mechanics*, vol. 10, pp. 111-129, 2016.

[3] A. Nessil, S. Larbi, H. Belhaneche and M. Malki, "Journal Bearings Lubrication Aspect Analysis Using Non-Newtonian Fluids", *Advances in Tribology*, vol. 2013, Article ID 212568, 9 pages, 2013.

[4] L. Paouris, R. Rahmani, S. Theodossiades, H. Rahnejat, G. Hunt and W. Barton," An Analytical Approach for Prediction of Elastohydrodynamic Friction with Inlet Shear Heating and Starvation," *Tribology Letters*, vol 64(10), Article number 10, 2016.

[5] J.Y. Jang, M.M. Khonsari and S. Bair, " On the Elastohydrodynamic Analysis of Shear-Thinning Fluids," *Mathematical, Physical and Engineering Sciences*, Vol. 463, No. 2088, pp. 3271-3290, 2007.

[6] H.M. Chu, W.L. Li and Y.P. Chang, "Thin film elastohydrodynamic lubrication a power-law fluid model," *Tribology international*, vol. 39(11), pp. 1474-1481, 2006.

[7] H.M. Chu, Y.P Cahang and W.L. Li, " Rheological Characteristics for Thin Film Elastohydrodynamic Lubrication with Non-Newtonian Lubricants," *Journal of Mechanics*, vol. 23 (4), pp. 359-366, 2007.

[8] G.D. Thakre, S.C. Sharma and S.P. Harsha, " A parametric investigation on the microelastohydrodynamic lubrication of power law fluid lubricated line contact," *Journal of Engineering Tribology*, vol. 229, Issue 10, pp. 1187-1205, 2015.

[9] S.M Karimi, M.N. Kinyanjui and M. Kimathi, " Surface Roughness and Density Effects in Thermal Elastohydrodynamic Lubrication Point Contacts," *American Journal of Mathematical and Computer Modelling*, Vol. 5, No. 3, pp. 89-96, 2020.

[10] A.F. Koura, M.E. Elhady and M.S. Metwally, " Numerical solution of Reynolds equation using differential transform method," *International Journal of Advanced Research (IJAR)*, vol. (6), pp. 729-737, 2018.

[11] S.M. Karimi, M. Kimathi, M. N. Kinyanjui, " Numerical Solution of Elastohydrodynamic Lubrication for Sliding/Rolling Bearing for Non-Newtonian Lubricant," *American Journal of Applied Mathematics*, Vol. 8, No. 5, pp. 257-264, 2020.

[12] J. Guegan, A. Kadiric, A. Gabelli and H. Spikes," The Relationship Between Friction and Film Thickness in EHD Point Contacts in the Presence of Longitudinal Roughness," *Tribology Letters*, vol. 64(33),Article number 33, 2016.

[13] M. Kaneta, P. Yang, I. Krupka et. al., " Fundamentals of thermal elastohydrodynamic lubrication in Si3N4 and steel circular contacts," *Journal of engineering tribology*, vol. 229 (8), pp. 929-939, 2015.

[14] L.M. Chu, H.C. Hsu, and C.H. Su, " Power law fluid model incoperaed into thin film elastohydrodynamic lubrication of circular contacts," *Transactions of the Canadian Society for Mechanical Engineering*, 39(3), pp.547-556, 2015.

[15] M.F.J Bohan, I.J. Fox, T.C. Claypole and D.T. Gethin, " Numerical modelling of elastohydrodynamic lubrication in soft contacts using non:Newtonian fluids," *International Journal of Numerical Methods for Heat and Fluid Flow*, Vol. 12, No. 4, pp. 494-511, 2002.

[16] P. Yang. Thermal EHL Theory. In: Wang Q.J., Chung YW,"(eds) Encyclopedia of Tribology," *Springer*, Boston, MA, 2013.

[17] N. Talekar and P. Kumar ," Steady State EHL Line Contact Analysis with Surface Roughness and Linear Piezo-viscosity," *Procedia Materials Science*, vol. 5, pp. 898-907, 2014.

[18] M. Masjedi and M.M. Khonsari," Film Thickness and Asperity Load Formulas for Line-Contact Elastohydrodynamic Lubrication With Provision for Surface Roughness," *ASME. J. Tribology*, vol. 134(1), Article ID 011503, 2012.

[19] A. Muminovic, N. Repcic and M. Colic," Thermo Elasto Hydrodynamic Lubrication Model of Mixed Friction,"*Procedia Engineering*, vol.69, pp. 49-56,2014.

[20] S. Thohura, M.M. Molla, M.M. and M.M.A. Sarker, " Numerical Simulation of Non-Newtonian Power-Law Fluid Flow in a Lid-Driven Skewed Cavity," *International Journal of Applied Computational Math*, vol. 5, no.14, pp. 1-29, 2019.

[21] D. Prasad and V. S. Sajja, " Non-Newtonian Lubrication of Asymmetric Rollers with Thermal and Inertia Effects," *Tribology Transactions*, vol. 59, no.5, pp. 818-830, 2016.

[22] J. Huo, J. Zhou, T. Li, Z. Meng and W. Sun, " Thermal EHL Characteristics Investigation on Axle Box Bearings of Railway Vehicle Based on Slicing Method," *Shock and Vibration*, Volume 2019, Article ID 6981482, 14 pages, 2019.

[23] A. Nessil, S. Larbi, H. Belhaneche and Maamar Malki, " Journal Bearings Lubrication Aspect Analysis Using Non-Newtonian Fluids," *Advances in Tribology*, Volume 2013, Article ID 212568, 9 pages, 2013.